Thermal stress modeling in cryosurgery

Yoed Rabin[a,*], Paul S. Steif[b]

[a]*Department of Mechanical Engineering, Technion—Israel Institute of Technology, Haifa 32000, Israel*
[b]*Department of Mechanical Engineering, Carnegie Mellon University, Pittsburgh, PA, USA*

Abstract

A new model of the mechanical stress development associated with an expanded freezing zone and its subsequent thawing is presented. The model is different in that it computes stresses properly by considering only strains that occur after solidification. A closed-form solution of the model is derived and results of a parametric study for typical parameters and conditions of cryosurgery around a spherical cryoprobe are presented. Results show that the stress distributions during the thawing stage are very different than those during freezing. Furthermore, it is shown that significant stresses remain in the frozen region during thawing, and even when the temperature distribution decays to the phase transition temperatures. The distributions are qualitatively consistent with limited cracking at the cryoprobe surface during freezing and large scale cracking during thawing, which were observed during validation testing of cryoprobes in water and gelatin solutions. © 2000 Elsevier Science Ltd. All rights reserved.

Keywords: Thermal stress; Phase change; Biological tissues; Cryosurgery; Modeling

1. Introduction

It is well known that freezing biological tissues can introduce severe damage. Sometimes this damage is intentional and desired, as in cryosurgery. In other situations, such as cryopreservation, this damage is an undesired byproduct. Mechanical stresses that develop during the freezing of biological solutions and tissues have been identified as one cause of tissue damage. In attempting to simulate cryosurgery and cryopreservation, mechanical stress development has been analyzed by a number of researchers (Rubinsky et al., 1980; Rubinsky, 1982; Lin et al., 1990; Gao et al., 1995; Rabin and Steif, 1996). While mechanical stress is one mechanism of tissue destruction in cryobiology applications (Ishiguro and Rubinsky, 1994; Hunt et al., 1994; Gao et al., 1995; Rabin et al., 1996, 1997a), there are other

---

* Corresponding author. Tel.: +972 4 829 2087; fax: +972 4 832 4533.
E-mail address: yoed@tx.technion.ac.il (Y. Rabin)

destruction mechanisms related to crystal growth and to mass transfer at the cellular level (Meryman, 1974; Mazur, 1984; Taylor, 1987).

Unfortunately, predictions of mechanical stresses are inconsistent with one important observation of tissue destruction: in cryopreservation applications, severe fractures often form at the early stages of thawing and not as commonly expected during freezing (Pegg, 1996). Comparable observations in the context of cryosurgical applications will be discussed in this paper. This inconsistency has prompted us to re-examine the assumptions underlying the models of freezing tissues presented to date. It is our belief, now, that behavior at the freezing front has not been properly modeled heretofore. Specifically, all stresses should be zero at an expanding freezing front. Any (volume preserving) strain that occurs while the material is still in the liquid state cannot contribute to the stress. Therefore, material which has just solidified at an expanding freezing front, must start with zero stress. We note that the zero stress condition at the freezing front has been well appreciated by workers in the area of metal solidification and casting (Boley and Weiner, 1963; Tien and Richmond, 1982; Heinlein et al., 1986; Zabaras and Ruan, 1990; Zabaras et al., 1991).

To simulate an idealized cryopreservation procedure, Rabin and Steif (1998) have recently analyzed the stresses associated with the inward freezing of a sphere. Their analysis included the condition of zero stresses at the freezing front; that condition, together with a proper accounting for the hydrostatic pressure that develops in the contained liquid region, resulted in dramatically different stress distributions during freezing than had previously been found. This has motivated the present paper which reconsiders the outward freezing problem simulative of cryosurgical procedures. A closed-form solution for this model is derived. Results reveal substantial increases in the thermal stresses during thawing, especially near the freezing front.

2. Observations of fracture during a simulated cryoprocedure

The observations of fracture reported here occurred during validation testing of a new liquid-nitrogen-based cryosurgical device, which is described in detail elsewhere (Rabin et al., 1997b). The experiments were performed in pure water and in 1.4% gelatin solution. Similar patterns of fractures were observed around cylindrical cryoprobes of length from 5 to 100 mm and diameters from 1.4 to 6 mm, as described below. Cooling rates of a few °C min^{-1} and up to about 200°C min^{-1} were measured at the cryoprobe surface. These cooling rates were maximum at higher temperatures and decay as the cryoprobe temperature approached the liquid nitrogen boiling temperature. An approximation of the cooling rate dependency in time is given in the discussion section.

A clear and well defined freezing front was observed as the cryoprobe temperature reached the freezing temperatures. As the cryoprobe continued cooling down a transparent frozen region developed. After some period of time, depending on the cryoprobe diameter and cooling rate, an opaque-milkish region started to form around the cryoprobe, well inside the frozen region. This opaque region, which contained some microcracks, was well defined and became thicker as the frozen region expanded. The thickness of this opaque region increased with the cooling rate; it was completely absent at very low cooling rates, and it approached one third of the frozen region (transparent) thickness for high cooling rates. This opaque region appeared stable in the sense that it grew steadily and slowly as the freezing process progressed.

The thawing stage was initiated by shutting off the coolant circulation. Very shortly after (on the order of s) severe macro-fractures developed, running through the entire frozen region in the radial direction. These macro fractures were observed prior to any significant reduction in the frozen region diameter due to thawing. Although the experimental observations described here are only qualitative, they are inconsistent with previous theoretical calculations (Rubinsky et al., 1980; Rubinsky, 1982; Lin

et al., 1990; Gao et al., 1995; Rabin and Steif, 1996) which all predict stresses to increase during freezing and decrease during thawing. The model presented in this paper shows why substantial tensile stresses develop during thawing.

Since similar observations of cracking during thawing were made for a relatively long cylindrical cryoprobe and for an almost spherical cryoprobe, it was deemed sufficient to model only the spherical geometry, which is simpler. Nevertheless, the major conclusions presented below are not expected to change substantially for a cylindrical cryoprobe. We also note, briefly, that the opaque zone around the cryoprobe, which contains micro-fractures, can be explained by the presence of plastic strains that occur when the stress reaches the yield strength of the material. It was indeed predicted by Rabin and Steif (1996) that plastic strains do develop around the cryoprobe. The plasticity effect in the current problem is assumed to be minor relative to the macro-fractures that develop during thawing and, therefore, is ignored in the present model.

3. Analysis

The problem analyzed here simulates the freezing of tissue around a spherical or nearly spherical cryoprobe, with the tissue surrounding the probe being large compared with probe itself. This is idealized by taking the probe to be a sphere, occupying the region $0 < r < R$; the surrounding tissue occupies the region $R < r < \infty$. The probe is made to follow a realistic cooling protocol which is set forth below. Our goal is to predict the stresses that develop as the frozen zone increases. Biological tissues freeze over a temperature range which is dependent on the chemical content of the cryotreated tissue and on its cooling history (Miller and Mazur, 1976; Taylor, 1987). When cooling quasi-statically, the phase transition temperature range is typically between 0 and $-22°C$ (assuming that body fluids behave like NaCl–H_2O mixture). It is assumed that the frozen tissue can sustain a significant mechanical load only after the completion of phase transition. Hence the solidus front, which is at $r = h$, is defined as the position which is instantaneously at the lower temperature boundary of phase transition. The solidus front location, as well as the temperature distribution, are assumed to be determined purely by the bioheat transfer problem, which is presented first, after which the distribution of stresses is determined.

3.1. Heat transfer problem

Heat transfer is assumed to be governed by the classical bioheat equation:

$$\frac{\partial H}{\partial t} = \nabla(k\nabla T) + \dot{w}_b(T_b - T) \tag{1}$$

where T is the temperature, H is the volumetric enthalpy, k is thermal conductivity, $\dot{w}_b$ is the production of the blood perfusion and its volumetric specific heat, and T_b is the blood temperature. The initial temperature distribution is assumed uniform and equal to the blood perfusion temperature. The heat transfer problem is solved numerically using the numerical scheme presented by Rabin and Shitzer (1998). The assumed phase transition temperature range and the thermophysical properties are listed in Table 1.

In order to simulate as closed as possible a typical cryosurgical cooling protocol, the following cryoprobe temperature forcing function is assumed:

$$T_R = T_b + (T_{LN2} - T_b)(1 - e^{-Dt}) \tag{2}$$

Table 1
Typical physical properties of frozen biological tissues

Poisson's ratio, v	0.33
Thermal expansion coefficient: $\beta_1 + \beta_2 T$	$\beta_1 = 60 \times 10^{-6}\,°C^{-1}$; $\beta_2 = 2.3 \times 10^{-7}\,°C^{-2}$
Elastic modulus, E	10 GPa
Blood perfusion temperature, T_b	37°C
Phase transition temperature range	$-22 - 0°C$
Thermal conductivity of the unfrozen tissue, k	$0.5\ W\ m^{-1}\,°C^{-1}$
Thermal conductivity of the frozen tissue, k	$2.0\ W\ m^{-1}\,°C^{-1}$
Specific heat of the unfrozen tissue	$3.6\ MJ\ m^{-3}\,°C^{-1}$
Specific heat of the frozen tissue	$1.8\ MJ\ m^{-3}\,°C^{-1}$
Latent heat	$250\ MJ\ m^{-3}$
Specific heat source of blood perfusion, $\dot{w}_b$	$25 \times 10^3\ s^{-1}$

where T_R is the cryoprobe temperature, T_{LN2} is the liquid nitrogen boiling temperature ($-196°C$ at 1 standard atm), and D is a cooling rate constant. Note that such a function is preferable to a step-like temperature change at the cryoprobe, or even a step-like change in the cryoprobe cooling rate, which are expected to result in unrealistically high thermal stresses. The range of typical cooling rates is discussed below. During thawing, the cryoprobe is assumed inactive which is represented by a mathematical condition of zero heat flux at the cryoprobe surface.

3.2. Solid mechanics problem

The analysis of stresses and strains is predicated on the following observations regarding the development of stresses. Since the fluid is taken to be inviscid, it can withstand no deviatoric stresses. We now argue that as the solid–liquid interface *advances steadily into the liquid zone*, material on the solid side of this interface must have zero stress. Consider first the case of no sudden expansion due to phase transition. In this case, the material on the solid side of the interface had zero stress at the previous instant (when it was liquid); since the interface is steadily advancing, there is no time during which the material could have strained in the solid state, and hence it must have zero stress in the solid state. Of course, as the interface progresses, elements that were earlier at the interface can with time develop stress. That stresses at an advancing interface must be zero is well appreciated in the modeling of metal solidification (see for example, Zabaras et al., 1991). By contrast, once the interface stops advancing (as cooling ceases at the cryoprobe in our problem), and even when it eventually moves backwards, the stresses at the solid side of the interface can evolve with time to become non-zero.

Now, consider the case when a sudden volume expansion due to phase transition can occur. Of course when the material is unconstrained, this strain can occur with no stresses. In fact, this sudden volume expansion will have no effect on the stresses in the solid region, because the volume change occurs through a sudden radial strain but no circumferential strain. The radial strain at the interface is allowed to take on any value, since the outward expansion is freely accommodated by the outer inviscid liquid.

The key physical quantities in the solid mechanics analysis, the displacements, strains and stresses, are functions of position and time, just as the temperature. We will be particularly careful in defining displacements and strains so as to permit a proper accounting for the stresses which develop in the solid region. Initially, the entire domain outside the cryoprobe is liquid. This state, prior to cooling at the cryoprobe, is the initial state (at time $t = 0$) from which all displacements and strains are measured. Let

a material point, which is initially at the point r, be located at the point r' at time t. Hence, r' is a function of r and of t. The radial displacement, u, is defined as the change of radial position of a material element, that is:

$$u(r,t) = r'(r,t) - r \tag{3}$$

Notice that all points are liquid at time $t = 0$, while a point may be either liquid or solid at time t. The radial strain ε_r and circumferential strain ε_θ are defined in the usual way with respect to the displacement u:

$$\varepsilon_r = \frac{\mathrm{d}u}{\mathrm{d}r}; \quad \varepsilon_\theta = \frac{u}{r} \tag{4}$$

Before defining the relations between stresses and strains (the constitutive relations), one important point needs to be made regarding the strains. Consider a point r which at time t has become solid. For the purposes of defining the stresses, what is its strain? Say that this element remained liquid up to the time t^*, at which time it solidified. In the time period $0 < t < t^*$, this element has strained, yet as a fluid, this strain can occur without stresses. Or, more precisely, strains involving no volume change (deviatoric strains) occur without stress, while any change in volume will require a pressure change (inversely proportional to the compressibility of the fluid). Hence, it will be necessary to keep track of the strain at which each element solidifies; only strain occurring thereafter contributes to deviatoric stress (the stress with the pressure subtracted off).

This background indicates the necessity of separating the stress components σ_{ij} into two parts, the deviatoric stress S_{ij} and the hydrostatic pressure p, in the standard fashion:

$$\sigma_{ij} = S_{ij} - p\delta_{ij} \tag{5}$$

Likewise the strains must be split into deviatoric e_{ij} and hydrostatic parts according to:

$$\varepsilon_{ij} = e_{ij} + \frac{1}{3}e\delta_{ij} \tag{6}$$

where δ_{ij} is the Kroneker index.

The liquid region can sustain hydrostatic pressure only. This liquid pressure has to be uniform, otherwise flow would occur. Moreover, since the pressure far away can be taken to be zero (or atmospheric, the base level not affecting the analysis), the pressure everywhere in the fluid must be zero.

Consider now the solid region. As pointed out above, it is necessary to keep track of how much straining occurs after solidification. With that idea in hand, though, it is still necessary to choose an appropriate stress–strain relation for the solid. Since cryosurgical procedures occur over a rather short period of time (on the order of min), viscous or relaxation effects can be neglected. This is in contrast to cryopreservation in which the material may have stresses for long periods of time during which relaxation is possible. Compression testing of frozen tissues (Rabin et al., 1996) indicate that the mechanical stress in the tissues is linearly related to the strain for small strains; as the strain increases to the level of approximately 0.005, however, the stress begins to fluctuate about a roughly constant value. This behavior, akin to plasticity, was attributed to the development of macro-cracking in the tissues (Rabin et al., 1997a). The effect of plasticity was analyzed by Rabin and Steif (1996, 1998); plastic straining should be confined to the region in the vicinity of the cryoprobe. The effect addressed in this paper—the rapid increase in stress when thawing begins—involves stresses at the outer portions of the frozen region; hence, plasticity is not critical to this effect. Accordingly, the present analysis neglects the plasticity and treats the frozen solid as elastic.

From the above considerations, we can express the deviatoric stresses in terms of the deviatoric strains as follows:

$$S_{ij} = 2G\left(e_{ij} - e_{ij}^*\right), \quad R < r < h \tag{7}$$

where G is the shear modulus, and e_{ij}^* is the deviatoric strain of the material element just after solidification; e_{ij}^* is a function of the position r. Notice that the total strain at a point r may change with time as the procedure continues, while the quantity e_{ij}^* has a single value at the point r. The shear modulus is related to the Young's modulus E and the Poisson ratio υ by:

$$G = \frac{E}{2(1+\upsilon)} \tag{8}$$

Notice that the material is assumed to be isotropic; consistent with this assumption, the thermal strains have zero deviatoric part (the thermal expansion is equal in all directions).

The hydrostatic pressure in the solid is given by:

$$p = -\kappa(e - e_{th}), \qquad R < r < h \tag{9}$$

where the bulk modulus, κ, is related to E and υ by:

$$\kappa = \frac{E}{3(1 - 2\upsilon)} \tag{10}$$

The volumetric thermal strain, e_{th}, is defined as:

$$e_{th} = 3\varepsilon_{th} = 3\int_0^\varphi \beta \, d\varphi \tag{11}$$

where ε_{th} is the linear thermal strain, β is the thermal expansion coefficient, and φ is the difference between the local temperature and the solidus temperature. The thermal expansion coefficient of frozen biological tissues can be approximated as linearly dependent on temperature, similar to polycrystalline ice (Rabin et al., 1998).

Finally, the mechanical equilibrium equation specialized to the spherically symmetric geometry is:

$$\frac{d\sigma_r}{dr} + \frac{2}{r}(\sigma_r - \sigma_\theta) = 0 \tag{12}$$

Consistent with zero pressure in the unfrozen region, a boundary condition of zero radial stress at the solidus front is assumed:

$$\sigma_r(h) = 0 \tag{13}$$

Note that, during freezing, the deviatoric stress at the solidus front is zero by definition in this new formulation, eqn (7). It follows that the hydrostatic pressure also equals zero at the solidus front, eqn (5).

Assuming that the elastic modulus of the cryoprobe is at least two orders of magnitude higher than that of the frozen tissue (stainless steel for example), the displacement at the cryoprobe outer surface is assumed to be solely governed by the cryoprobe thermal strain:

$$\frac{u(R)}{R} = \varepsilon_R \tag{14}$$

where ε_R is the thermal strain of the cryoprobe at its outer surface.

To reduce the above set of equations to a form which can readily be solved numerically, the function $g(r)$ is introduced:

$$g(r) \equiv \frac{3}{2}e_r^* = (\varepsilon_r - \varepsilon_\theta)^*, \quad @r = h \tag{15}$$

We recapitulate the significance of this term: the function $g(r)$ can be seen as a history function of the process, and proportional to the deviatoric strain which had developed at the point r up to the instant of its freezing. This strain should not be counted in determining the deviatoric stresses in the frozen material.

It is now possible to express S_r and p in terms of the radial displacement, u, and the various other known quantities, and to substitute into the equation of equilibrium, eqn (12); the result is:

$$(4G + 3\kappa)\frac{\mathrm{d}}{\mathrm{d}r}\left(\frac{\mathrm{d}u}{\mathrm{d}r} + 2\frac{u}{r}\right) - 4G\frac{1}{r^3}\frac{\mathrm{d}}{\mathrm{d}r}(r^3 g) - 3\kappa\frac{\mathrm{d}e_{\mathrm{th}}}{\mathrm{d}r} = 0 \tag{16}$$

The solution of this equation is:

$$u = \frac{3\kappa}{4G + 3\kappa}\frac{1}{r^2}\int_R^r e_{\mathrm{th}}r^2\,\mathrm{d}r + \frac{4G}{4G + 3\kappa}\left[r\int_R^r \frac{g}{r}\mathrm{d}r - \frac{g_R}{3}\left(r - \frac{R^3}{r^2}\right)\right] + B_1 r + \frac{B_2}{r^2} \tag{17}$$

where B_1 and B_2 are integration constants and g_R is the initial value of the function g at the cryoprobe surface. Substituting the displacement given by eqn (17), into the strain-displacement relations, eqn (4), and applying the zero hydrostatic pressure condition at the solidus front, eqn (13), one finds the integration constant B_1 to be:

$$B_1 = -\frac{4G}{4G + 3\kappa}\left[\int_R^h \frac{g}{r}\mathrm{d}r + \frac{g_h - g_R}{3}\right] \tag{18}$$

where g_h is the value of the function g at the current solidus front location. Integration constant B_2 is found by applying boundary condition, eqn (14), into the displacement solution, eqn (17):

$$B_2 = (\varepsilon_R - B_1)R^3 \tag{19}$$

At any instant in time, the history function, g, is known everywhere in the solid domain except at the current solidus front location. However, this function can be expressed at the current time instant by substituting eqns (4) and (17) into eqn (15):

$$g_h = -\frac{1}{h^3}\left(\frac{4G}{3\kappa}R^3 g_R + \frac{4G + 3\kappa}{\kappa}B_2 + 3\int_R^h e_{\mathrm{th}}r^2\,\mathrm{d}r\right) \tag{20}$$

The solution is now well defined implicitly and has to be solved by a predictor-corrector procedure for the history function value at the solidus front, g_h, at the current time point. This is done as follows: (i) the value g_h is predicted (0 at the beginning of freezing or the value at the previous time instant elsewhere); (ii) the constant B_1 is calculated from eqn (18); (iii) the constant B_2 is calculated from eqn (19); (iv) the value of h_h is corrected using eqn (20). Stages (ii)–(iv) are repeated until the value g_h converges. It is emphasized that, although a close form solution in space is presented, it has to be calculated incrementally in time for the strain history function, g.

Final forms for the deviatoric stress and hydrostatic pressure in the frozen region are, respectively:

$$S_r = -\frac{1}{2}S_\theta = \frac{4G\kappa}{4G + 3\kappa}\left[-\frac{3}{r^3}\int_R^r e_{th}r^2\,dr + e_{th} - g\right] - \frac{16}{3}\frac{G^2}{4G + 3\kappa}\frac{R^3}{r^3}g_R - 4G\frac{B_2}{r^3} \tag{21}$$

and

$$p = -\frac{4G\kappa}{4G + 3\kappa}\left[3\int_R^r \frac{g}{r}\,dr + g - g_R - e_{th}\right] - 3\kappa B_1 \tag{22}$$

Consider now the thawing stage. The formulation presented above is valid during thawing as well. It is now possible, however, for some stress components to be non-zero at the solidus front. Recall that the deviatoric stresses arise from any difference between the strains at the current instant and the strains at which that material first froze. During the cooling stage, the solidus front is propagating outwards continuously; at all times the material at the solidus front *has just frozen*. As thawing begins, the solidus front ceases to propagate outward, but the strains everywhere, including at the front, continue to evolve. Thus, the strain at the front begins to differ from the value it had when first freezing, and deviatoric stresses can develop.

We continue to invoke the condition of zero radial stress, eqn (13), at the solidus front since the fluid region continues to have zero stress. During the thawing stage we no longer need to calculate the function *g*; its distribution in the solid region was determined during the freezing stage. This leads to a change in the first constant of integration:

$$B_1 = \frac{1}{3\kappa h^3 + 4GR^3}\left[\frac{12G\kappa}{4G + 3\kappa}\int_R^h\left(e_{th}r^2 - h^3\frac{g}{r}\right)dr + 4G\varepsilon_p R^3\right] + \frac{4Gg_R}{3(4G + 3\kappa)} \tag{23}$$

4. Results and discussion

Parametric studies were performed by a spherical cryoprobe with radius 2.5 mm, using space intervals of 0.05 mm and time intervals of 2.5×10^{-3} s, for a freezing period of up to 20 min. The cryoprobe was assumed to be stainless steel, having an average thermal expansion coefficient of $2 \times 10^{-5}\,°C^{-1}$. Typical thermophysical properties of the biological tissues were assumed in this study as listed in Table 1.

Fig. 1 shows the cryoprobe temperature forcing function using cooling rate constants, *D*, of 0.01, 0.02, and 0.03, which are assumed to correspond to low, average, and high power cryoprobes, respectively. Fig. 2 shows the solidus front location for a freezing/thawing cycle consisting of 20 min of cooling followed by free thawing driven by heat transfer from the unfrozen region (the cryoprobe is inactive during the thawing stage). It can be seen from Fig. 2 that the dependency of the solidus front location in the cryoprobe cooling rate constant, *D*, is significant in the short term only. It can also be seen that the solidus front propagates very fast backwards during the beginning of the thawing stage. By contrast, the liquidus front (not shown), which is defined by the upper boundary of the phase transition temperature range, does not move so rapidly backwards. In fact, the thickness of the phase transition layer, defined by the liquidus and solidus fronts, increases significantly during thawing, and may occupy a large portion of the hollow sphere defined by the liquidus front and the cryoprobe surface.

Fig. 3 shows the temperature distributions in the solid for different solidus front locations, during freezing and thawing, which are the results from a single freeze/thaw cycle. It can be seen from Fig. 3 that very different temperature distributions prevail during freezing and thawing, for any given interface location. The temperature distribution during thawing appears far more moderate than during freezing.
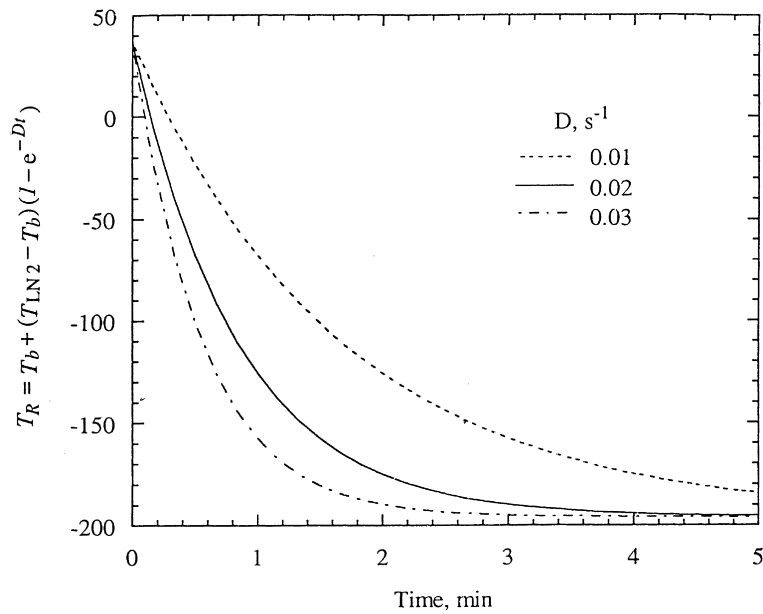
Fig. 1. Cryoprobe temperature forcing function.

The distributions in the total stress components (normalized by the elasticity modulus) are depicted in Figs. 4 and 5 for a number of positions of the solidus front. Similarly, the deviatoric stress components are shown in Fig. 6. The dashed curves correspond to freezing, and the solid curves correspond to thawing. There is a rather dramatic difference between freezing and thawing; these differences can be attributed to the now proper accounting for the strain that contributes to stress in the solid phase. As
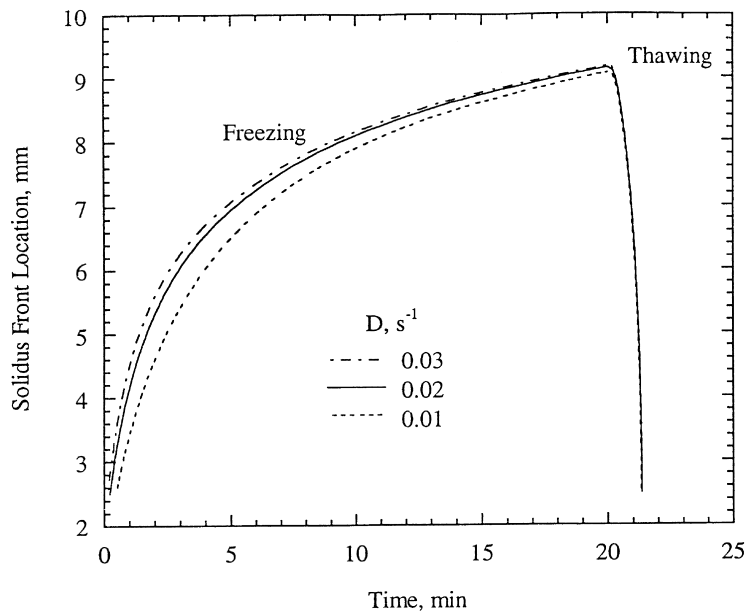
Fig. 2. Time evolution of solidus front location *h*.
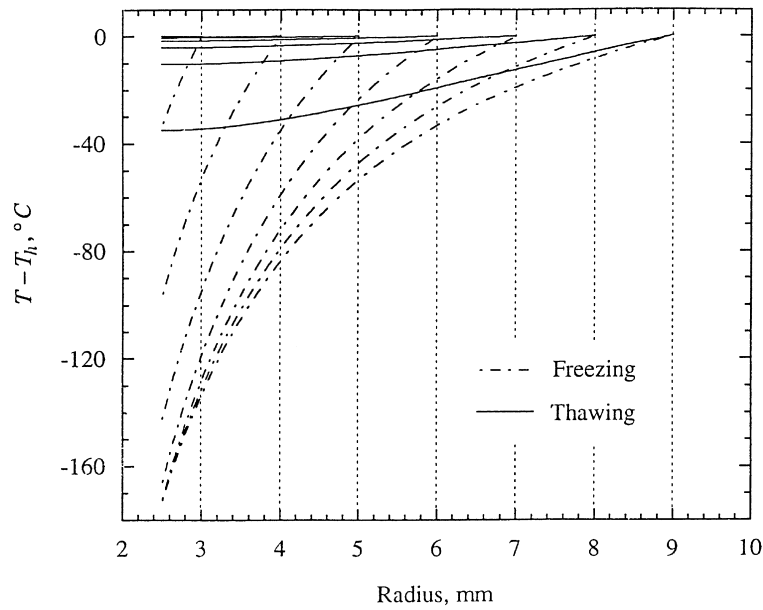
Fig. 3. Temperature distribution at various time instants (indicated by solidus front location) during freezing and thawing, where T_h is the solidus front temperature.

required by this theory, both stresses are zero at the solidus front during freezing. By contrast, only the radial stress σ_r is zero at the solidus front during thawing. The radial stress is always compressive, while the circumferential stress σ_θ can be compressive or tensile.
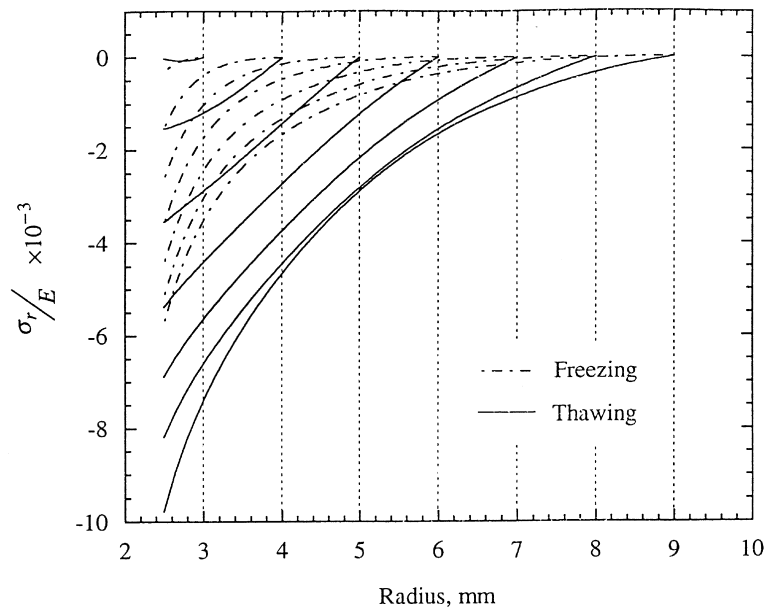

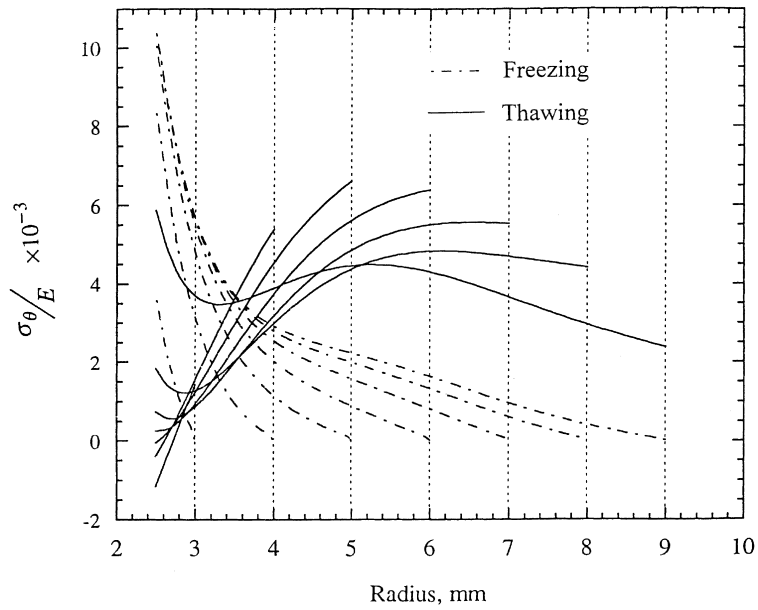Fig. 4. Radial strain at various time instants during freezing and thawing.

Fig. 5. Circumferential strain at various time instants during freezing and thawing.

From these distributions one can draw only qualitative conclusions regarding failure, since departures from idealized elastic behavior will eventually occur. For example, the material can deform plastically with micro-cracks appearing (as found from compression testing of frozen tissues by Rabin et al., 1996, 1997a); under tensile stresses, one expects macroscopic cracks to form. In either case, the stress
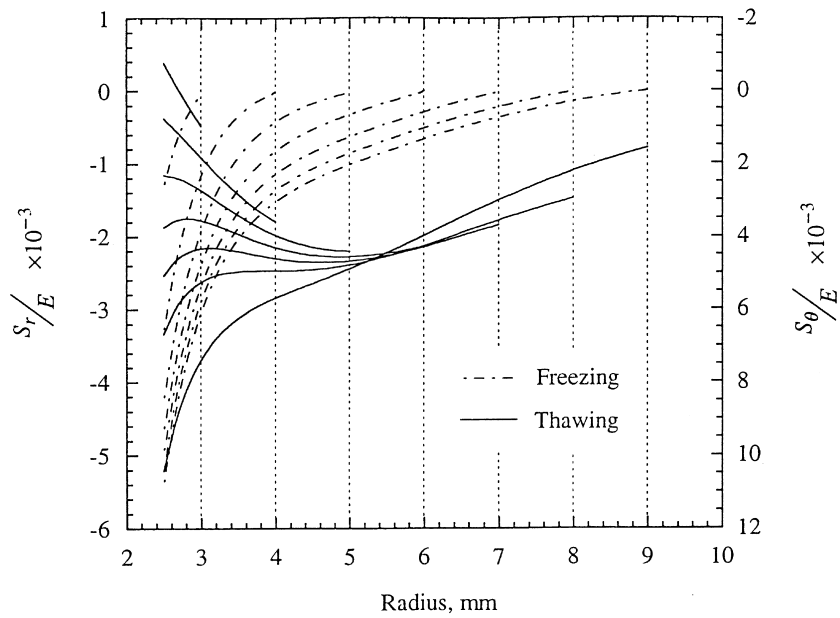

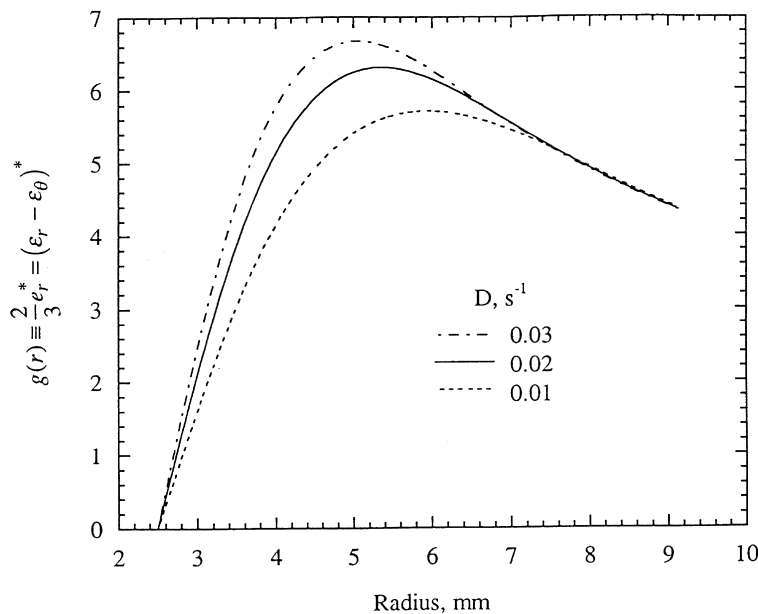Fig. 6. Deviatoric stress components during freezing and thawing at various time instants.

Fig. 7. Function g as a function of the radius for different cooling rate constants.

distributions will depart from those predicted here once plasticity or cracking occur. With this caution in mind, one can see from the plot of σ_θ that cracks, should they appear during freezing, will do so near the probe. Since the tensile stress drops off rapidly with radius, these cracks should be confined to the probe region. This is observed qualitatively in our experiments. On the other hand, once thawing initiates there is a rapid rise in the tensile stress in the circumferential direction, which quickly becomes maximum near the solidus front. Since the tensile stresses do not drop off rapidly with radius (they are substantial over much of the frozen region, in contrast to freezing), one would not be surprised to find cracks throughout the frozen region; again, this was observed. The radial stress, however, is always compressive but its magnitude increases significantly during thawing. Note that the rapid change in deviatoric stress distribution at the beginning of thawing is associated with extremely high strain rates; the strength of the frozen material is expected to decrease with increase in the strain rate.

The function g shown in Fig. 7, is proportional to the strain difference which existed at a point in space when the material there solidified. The relatively high values of this function explain why the stresses get high values even when the temperature distribution decays to the solidus front temperature. The effect of the cryoprobe cooling rate on the function g can also be seen in Fig. 7 which indicates that the same general distribution of stresses is expected for relatively low and relatively high power cryoprobes.

5. Summary and conclusions

A closed-form solution of the thermal stresses associated with an expanded freezing region and subsequent thawing is presented. The solution is based on a more careful accounting for the strains that contribute to the stress, namely including only those strains that occur after solidification. A parametric study has been performed for typical parameters and conditions of cryosurgery around a spherical cryoprobe. Results have shown that the stress distributions during the thawing stage are very different

than those during freezing. Furthermore, it is shown that significant stresses remain in the frozen region during thawing, and even when the temperature distribution in the frozen region decays to the solidus temperature. The distributions are qualitatively consistent with limited cracking at the cryoprobe surface during freezing and large scale cracking during thawing.

References

Boley, B.A., Weiner, J.H., 1963. Elasto-plastic thermal stress in a solidifying body. J. Mech Phys. Solids 11, 145–154.

Gao, D.Y., Lin, S., Watson, P.F., Critser, J.K., 1995. Fracture phenomena in an isotonic salt solution during freezing and their elimination using glycerol. Cryobiology 32, 270–284.

Heinlein, M., Mukherjee, S., Richmond, O., 1986. A boundary element method analysis of temperature fields and stresses during solidification. Acta Mechanica 59, 59–81.

Hunt, C.J., Song, Y.C., Bateson, A.J., Pegg, E.D., 1994. Fractures in cryopreserved arteries. Cryobiology 31, 506–515.

Ishiguro, H., Rubinsky, B., 1994. Mechanical interaction between ice crystals and red blood cells during directional solidification. Cryobiology 31, 483–500.

Lin, S., Gao, D.Y., Yu, X.C., 1990. Thermal stress induced by water solidification in a cylindrical tube. ASME Journal Heat Transfer 112, 1079–1082.

Mazur, P., 1984. Freezing of living cells: mechanisms and implications. Am. J. Physiol. 247, C125–C142.

Meryman, H.T., 1974. Freezing injury and its prevention in living cells. Annual Review of Biophysics and Bioengineering 3, 341–363.

Miller, R.H., Mazur, P., 1976. Survival of frozen-thawed human red cells as a function of cooling and warming velocities. Cryobiology 13, 404–414.

Pegg, D.E., 1996. Problems in the cryopreservation of tissues and organs. Cryobiology 33 (6), 658–659.

Rabin, Y., Shitzer, A., 1998. Multidimensional numerical solution for the freezing problem during cryosurgery. ASME Journal of Biomechanical Engineering 120 (1), 32–37.

Rabin, Y., Steif, P.S., 1996. Analysis of thermal stresses around cryosurgical probe. Cryobiology 33, 276–290.

Rabin, Y., Steif, P.S., 1998. Thermal stresses in a freezing sphere and its application to cryobiology. ASME Journal of Applied Mechanics 65 (2), 328–333.

Rabin, Y., Julian, T.B., Wolmark, N., 1997b. A compact cryosurgical apparatus for minimal-invasive cryosurgery. Biomedical Instrumentation and Technology 31, 251–258.

Rabin, Y., Taylor, M.J., Wolmark, N., 1998. Thermal expansion measurements of frozen biological tissues at cryogenic temperatures. ASME Journal of Biomechanical Engineering 120 (2), 259–266.

Rabin, Y., Steif, P.S., Taylor, M.J., Julian, T.B., Wolmark, N., 1996. An experimental study of the mechanical response of frozen biological tissues at cryogenic temperatures. Cryobiology 33, 472–482.

Rabin, Y., Olson, P., Taylor, M.J., Steif, P.S., Julian, T.B., Wolmark, N., 1997a. Gross damage accumulation in frozen rabbit liver due to mechanical stress at cryogenic temperatures. Cryobiology 34, 394–405.

Rubinsky, B., 1982. Thermal stress during solidification. ASME Journal of Heat Transfer 104, 196–199.

Rubinsky, B., Cravalho, E.G., Mikic, B., 1980. Thermal stress in frozen organs. Cryobiology 17, 66–73.

Taylor, M.J., 1987. Physico-chemical principles in low temperature biology. In: Grout, B.W.W., Morris, G.J. (Eds.), The Effect of Low Temperatures on Biological Systems. pp. 3–71.

Tien, R.H., Richmond, O., 1982. Theory of maximum tensile stresses in the solidifying shell of a constrained rectangular casting. ASME Journal of Applied Mechanics 49, 481–486.

Zabaras, N., Ruan, Y., 1990. Front tracking thermomechanical model for hypoelastic-viscoplastic behavior in a solidifying body. Computer Methods in Applied Mechanics and Engineering 81, 333–364.

Zabaras, N., Ruan, Y., Richmond, O., 1991. On the calculation of deformations and stresses during axially symmetric solidification. ASME Journal of Applied Mechanics 58, 865–871.